

Projective Ranking-based GNN Evasion Attacks

He Zhang, Xingliang Yuan, Chuan Zhou, Shirui Pan

Abstract—Graph neural networks (GNNs) offer promising learning methods for graph-related tasks. However, GNNs are at risk of adversarial attacks. Two primary limitations of the current evasion attack methods are highlighted: (1) The current *GradArgmax* ignores the “long-term” benefit of the perturbation. It is faced with zero-gradient and invalid benefit estimates in certain situations. (2) In the reinforcement learning-based attack methods, the learned attack strategies might not be transferable when the attack budget changes. To this end, we first formulate the perturbation space and propose an evaluation framework and the projective ranking method. We aim to learn a powerful attack strategy then adapt it as little as possible to generate adversarial samples under dynamic budget settings. In our method, based on mutual information, we rank and assess the attack benefits of each perturbation for an effective attack strategy. By projecting the strategy, our method dramatically minimizes the cost of learning a new attack strategy when the attack budget changes. In the comparative assessment with *GradArgmax* and *RL-S2V*, the results show our method owns high attack performance and effective transferability. The visualization of our method also reveals various attack patterns in the generation of adversarial samples.

Index Terms—Adversarial attacks, graph neural networks, graph classification.

1 INTRODUCTION

GRAPHS consist of nodes and edges defined between these nodes. As an abstract data type, graphs have powerful modelling capabilities. By extracting attributes from entities and describing their relationships, graphs can represent a range of objects or technical systems in real-world situations, such as drug molecules [1], biological networks [2], and traffic networks [3], [4]. Graph neural networks (GNNs) have proven to be effective graph learning methods [5] for exploring graph data and have demonstrated promising performance on node classification [6], [7], link prediction [8], anomaly detection [9], [10], and graph classification [11]. For example, in biological chemistry, the GNNs are engaged in recognizing the chemical properties of molecules.

In practice, GNNs raise urgent security concerns, although they have garnered considerable attention in the context of complex graph-structured data applications [12], [13], [14], [15]. Generally, graph neural networks are regarded as the generalization of deep neural networks into graph data. However, GNNs inherit the vulnerability of deep neural networks despite possessing adequate expressive power. Several recent studies demonstrate that adversaries can attack GNNs [16], [17], [18], [19], [20]. Among others, evasion attacks [21], [22] are notoriously dangerous. Attackers could perturb test samples to generate adversarial samples of a victim model trained on original clean data. On adversarial samples, the victim model will give incorrect results, different from those of clean samples.

Prior work on GNN evasion attacks has demonstrated that well-designed slight perturbations are able to significantly degrade the performance of the victim models [21].

- H. Zhang and S. Pan are with the Department of Data Science and AI, Faculty of IT, Monash University, Clayton, VIC 3800, Australia
- X. Yuan is with the Department of Software Systems and Cybersecurity, Faculty of IT, Monash University, Clayton, VIC 3800, Australia
E-mail: {he.zhang1, xingliang.yuan, shirui.pan}@monash.edu
- C. Zhou is with Academy of Mathematics and Systems Science, Chinese Academy of Sciences, China. Email: zhouchuan@amss.ac.cn;
- Corresponding Author: Xingliang Yuan and Shirui Pan.

This type of attack is tricky since adversarial samples are similar to clean samples in appearance [17]. Adding a few elaborate adversarial edges can dramatically reduce the classification accuracy of the victim models [22]. To create an adversarial example, attackers can change the features of few nodes or add/remove a few edges in a clean graph. A *budget* k with positive integer values controls the number of these perturbation operations to make their perturbations stealthy. Moreover, once the models are deployed, it is practical for attackers to launch the evasion attacks at any time [19].

The existing studies of evasion attacks on the GNN models mainly focus on node classification and link prediction, while few of them are designed for graph classification [16], [17], [19]. We note there are some *limitations* in those methods for graph classification, which need to be solved to improve the attack practicality.

- In the vanilla gradient-based attack method *GradArgmax* [21], the greedy mechanism uses the gradient on the graph in the perturbation process to make the perturbation decision. Although the gradient information could approximate the attack benefit to some extent, it ignores the long-term benefit of operation at each step [21]. Moreover, *GradArgmax* is not efficient since it needs the up-to-date gradient information to complete each step of all the perturbation operations.
- Attack methods [21], [23] use reinforcement learning (RL) to perturb clean samples and use the final predicted result on adversarial samples to estimate the attack benefit. When the perturbation budget changes, they have to be retrained to learn an attack strategy suitable for the new budget. In addition, we observe that *RL-S2V* [21], a known attack method, does not appear to be able to generate adversarial samples in high attack success rates when the perturbation budget increases [23].

Motivated by these observations, we summarize the

challenges in building an effective evasion attack against GNNs for graph classification: (1) *in the generation of powerful adversarial samples, how to measure the attack benefits of each operation based on the clean graph*, and (2) *how to adapt the learned attack strategy to changed perturbation settings (e.g., budget) with least effort*.

To address these challenges, we first formulate the perturbation space composed of all possible perturbation operations and present four properties of it. Then, we propose an evaluation framework consisting of three principles decomposed from the adversary’s expectation. We use these three principles as the design goal of our method and employ them to evaluate typical evasion attack methods. In our evaluation framework, we consider a basic fact in the evasion attack: an intelligent attacker always expects to choose the perturbation operation which will bring the most significant attack benefit at each perturbation step. This fact includes three critical principles for evasion attack: *attack benefit*, *operation ranking* and *baseline graph*. Finally, we propose the projective ranking method as an instantiation under the evaluation framework.

In our method, we expect to find a suitable metric that considers the attack benefits of each operation to rank them and then use this ranking directly to generate adversarial samples under different perturbation budget settings. Towards the first challenge, we employ the mutual information (MI) between elements of perturbation space and attackers’ goals as a measure to evaluate the importance of each possible operation. We regard the perturbation space ranking as the learned attack strategy. Inspired by the projected gradient descent method, we propose to project the learned attack strategy into practical attackers’ perturbations with the specified budget for the second challenge. Through this projection operation, the adjustment cost of the learned attack strategy is almost zero.

Our contributions are summarized below:

- We formulate the perturbation space and its four properties, and we propose an evaluation framework for evasion attack methods and analyze typical methods from the principles of the framework.
- We propose the projective ranking method. We first employ the mutual information to measure the attack benefits of a perturbation operation towards strong attack performance, then use the projection operation to reduce the cost of the strategy adaptation process by considering the transferability of attack strategies.
- We conduct evaluations on several real world datasets and a synthesized dataset, and our attack method achieves high attack performance and effective transferability. The visualization of adversarial samples present various attack patterns and reveals the vulnerability of the victim model.

In this paper, we review different attack methods for graph classification in Section 2 and introduce the graph classification and evasion attacks in Section 3. In Section 4, we first formulate the perturbation space and show its four properties. Then we propose the evaluation framework of evasion attack methods and show the instantiation design of our method. Next, we show the detail of the projective ranking method. In Section 5, we use the evaluation frame-

work to make a comparison evaluation of typical methods. In Section 6, we experimentally demonstrate the high attack performance and effective transferability of our method, and the attack patterns in our adversarial samples reveal the weaknesses of the victim model. Finally, we show the conclusion and discuss the future works in Section 7.

2 RELATED WORK

Current research shows that graph neural networks are vulnerable to adversarial attacks. According to the intention of attackers, the adversarial attack methods for graph classification include evasion attacks, backdoor attacks, and poisoning attacks.

2.1 Evasion Attack Methods on GNNs

Evasion attacks perturb the inputs of the GNNs during their inference phase and intend to degrade the performance of the victim model. Hence, the more the classification accuracy of the victim model decreases, the better the performance of an attack method. As the most intuitive approach, *RandomSampling* randomly perturbs the graph structure or nodes’ features of clean graphs to generate adversarial samples. However, the attack performance of this method is lower than adding well-designed perturbations. In the *GradArgmax* method, the attackers own the ability to access the victim model. They first calculate the gradient information of the loss function on each possible perturbation operation, then use the gradient information to choose the perturbation operation that maximizes the loss of the victim model.

To better describe the perturbations on graph data, Dai et al. [21] proposed to employ the Markov decision process to model the whole perturbation process and use reinforcement learning to obtain an attack strategy on current clean samples. The graph data in the perturbation process is modeled as the state of reinforcement learning. The action space comprises all perturbation operations in the current state, and the final attack result defines the reward function. Benefiting from the modelling and learning ability of reinforcement learning, the attack performance of *RL-S2V* outperforms that of *RandSampling* and *GradArgmax* on synthetic data [21].

To improve the stealthiness of attack, Ma et al. proposed *ReWatt* to redefine the action space of reinforcement learning [23]. The perturbations generated by *ReWatt* are more unnoticeable since the edge numbers of adversarial samples are equal to those of clean samples. Besides the above attack methods, the attackers could also attack the components of GNNs if they know a specified operation is included in the victim model. For example, some methods introduce hierarchical pooling operations in the models, which selects typical nodes to compress the node number and determine the structure of the coarse graph [24], [25], [26].

Tang et al. proposed to attack the selecting operation in pooling operation [27]. By training a surrogate model with hierarchical pooling on some clean data, the attackers obtain the selecting function that simulates the victim model’s hierarchical pooling. Based on this selection function, the attackers could obtain the adversarial samples that invalidate

TABLE 1
Evasion Attack Methods for Graph Classification.

Method	Decision-making information	Operations		Attack Goal	Transferability of Attack Strategy	
		Edges	Features		Unseen samples	Budget
Rand*	Random	Add/Remove	-	Untargeted attack	-	-
GradArgmax	Gradient of loss function	Add/Remove	-	Untargeted attack	-	-
RL-S2V	Reward in RL	Add	-	Untargeted/Targeted attack	✓	-
ReWatt	Reward in RL	Rewrite	-	Untargeted/Targeted attack	✓	-
HGP*	Gradient of selection function	Add/Remove	modify	Untargeted attack	-	-
Ours	Mutual information	Add	-	Untargeted/Targeted attack	✓	✓

* Rand means the *RandomSampling*, HGP means the method for attacking the pooling operation in Hierarchical Graph Pooling Neural Networks.

the pooling in the victim model. However, this method may not be available for attacking models that employ global pooling operations. A comparison of representative evasion attack methods are summarized in Table 1.

2.2 Differences in Evasion Attacks

In addition to the differences in technical methods, the evasion attack methods also have differences in perturbation space, the definition of imperceptible perturbations, the attacker’s knowledge, and the attack goal. In the aspect of perturbation space, the attackers usually make perturbations by adding fake nodes with the fake features [28], modifying node features [29], adding or deleting edges [30]. In graph classification evasion attacks, *ReWatt*, *RL-S2V*, *RandSampling* and *GradArgmax* only modify graph structure. The attack method in [27] makes perturbations in node features or graph structure.

In the aspect of imperceptible perturbations, the distance between the original clean graph and the modified adversarial graph is usually limited by the perturbation budget, which is defined as the number of nodes modified or distance of feature vectors, or the number of edges modified by adding/deleting/rewriting. In the aspect of attackers’ knowledge, based on how much information an attacker knows about the victim model, the attack methods are generally divided into white-box, grey-box, and black-box attack. A white-box attack means the attackers can access all information about the victim model like architecture, parameters, training input, and labels. Grey-box attack indicates that only limited information about the victim model, like training data labels, is available. As the strictest setting, the black-box attack only allows attackers to do queries of samples for output or labels [16].

In graph classification evasion attack, *GradArgmax* is a white-box attack method, *RL-S2V* and *ReWatt* are typical black-box attack methods based on reinforcement learning. In the aspect of the attackers’ goal, the attacks are divided into untargeted attacks and targeted attacks. In an untargeted attack, the attackers expect the victim model to classify the adversarial samples into labels different from their original labels. As a more strict attack goal, targeted attacks attempt to fool the victim model by specifying the output categories of the adversarial samples.

2.3 Poisoning and Backdoor Attacks on GNNs

Besides evasion attacks, another two typical adversarial attacks on GNN models are poisoning attacks and backdoor attacks. The poisoning attacks [31] suppose the attackers

own the ability to poison training data and label. In this way, the performance of the GNN models trained on poisoned data will degrade dramatically on clean samples. In backdoor attacks [32], [33], the attackers inject a fixed or adaptive trigger into clean training data and change their labels to the desired categories. As a result, the models trained on these data performs well on the clean samples but predicts the desired labels once the well-designed trigger is injected into the clean samples.

3 PRELIMINARY

3.1 Graph Classification

Assuming $G = \{\mathcal{V}, \mathcal{E}\}$ is a graph, where $\mathcal{V} = \{v_1, \dots, v_{|\mathcal{V}|}\}$ is the set of nodes, $\mathcal{E} = \{e_1, \dots, e_{|\mathcal{E}|}\}$ is the set of edges of graph G . The edges set \mathcal{E} describes the structural information of G . It can also be expressed as the adjacency matrix $A \in \{0, 1\}^{|\mathcal{V}| \times |\mathcal{V}|}$, where $A_{ij} = 1$ means the existence of the edge from v_i to v_j , otherwise $A_{ij} = 0$. The features associated with nodes are expressed as matrix $X \in \mathbb{R}^{|\mathcal{V}| \times d}$, where the i -th row of X is the features of node v_i and d is the dimension of features. So a graph can also be expressed as $G = \{A, X\}$.

In the graph classification, a set of graphs is denoted by $\mathcal{G} = \{G_i\}_{i=1}^N$ and a label $y_i \in \mathcal{Y} = \{1, 2, \dots, Y\}$ is associated with each graph G_i , where N is the number of graphs and Y is number of categories. The dataset $\mathcal{D} = \{(G_i, y_i)\}_{i=1}^N$ is composed of pairs of graph and its label. In graph learning, the classifier $f \in \mathcal{F} : \mathcal{G} \rightarrow \mathcal{Y}$ is trained and expected to learn the mapping from graph G to its label y with optimal parameters θ that minimize the below loss function:

$$\mathcal{L} = \frac{1}{N} \sum_{i=1}^N L(f_\theta(G_i), y_i), \tag{1}$$

where $L(\cdot, \cdot)$ is used to measure the distance between the predicted and ground-truth labels. A general instance of $L(\cdot, \cdot)$ is the cross-entropy function.

3.2 Graph Neural Networks Model

The graph neural networks (GNNs) is a family of architectures of neural networks that are designed to process graph data $G = \{\mathcal{V}, \mathcal{E}\}$. These models iteratively update the expression of nodes by message passing and aggregation as below [34]:

$$m_v^{t+1} = \sum_{w \in \mathcal{N}(v)} M_t(h_v^t, h_w^t, e_{vw}), \tag{2}$$

$$h_v^{t+1} = U_t(h_v^t, m_v^{t+1}), \tag{3}$$

where $N(v)$ is the set of neighbours of node v in graph G , h_v^t means the hidden expression of node v at time $t \in \{1, 2, \dots, T\}$ and e_{vw} is the features of the edge from node v to node w . $M_t(\cdot, \cdot, \cdot)$ is the message functions and $U_t(\cdot, \cdot)$ is the vertex expression updating functions. After the message passing phase, the expression of whole graph G is obtained by the readout operation:

$$h_G = R\left(\left\{h_v^T \mid v \in G\right\}\right) \quad (4)$$

where $R(\cdot)$ is the readout operation, and it is invariant to permutations of the nodes. A general instance of $R(\cdot)$ is the *max-pooling* or *sum-pooling*.

In graph classification, the model f_θ based on the above architecture is generally trained under an inductive learning setting, in which the classifier learns on training data \mathcal{D}_{train} and then make graph label prediction on test data \mathcal{D}_{test} .

3.3 Problem Formulation

Assuming a GNN model f_θ is trained on clean graph samples and then employed to predict the category of graph data $\mathcal{D} = \{G_j\}_1^M$. In evasion attacks, an attacker \mathcal{T} attempts to make unnoticeable perturbations on the original G to degrade the performance of this victim model f_θ . We use $\mathcal{T}_f(G)$ to indicate the attacker's perturbation on G which is specifically designed for the classifier f_θ . In untargeted evasion attacks, the attackers expect the predicted category of an adversarial sample is different from its true category. More precisely, the objective of *untargeted evasion attacks* on the victim model f_θ is

$$\begin{aligned} \max_{\hat{G}} \quad & \sum_{j=1}^M \mathbb{I}\left(f_\theta(\hat{G}_j) \neq y_j\right) \\ \text{s.t.} \quad & \hat{G} = \mathcal{T}_f(G) \\ & \mathcal{I}(\hat{G}, G; k) = 1. \end{aligned} \quad (5)$$

Here \hat{G} is the adversarial sample generated from the clean sample G , and $\mathbb{I}(\cdot)$ is the binary indicator function. k is the perturbation budget of \mathcal{T}_f . Given specific k , $\mathcal{I}(\cdot, \cdot; k)$ is a similarity measure function whose output is 1 when two input graph samples are semantically the same and 0 otherwise. Particularly, in targeted evasion attacks, the attackers expect the predicted category is a specified category y_t , which is different from its true category y_j . The objective of *targeted evasion attacks* is

$$\begin{aligned} \max_{\hat{G}} \quad & \sum_{j=1}^M \mathbb{I}\left(f_\theta(\hat{G}_j) = y_t\right) \\ \text{s.t.} \quad & \hat{G} = \mathcal{T}_f(G) \\ & \mathcal{I}(\hat{G}, G; k) = 1, \\ & y_t \neq y_j. \end{aligned} \quad (6)$$

Note. The probability function $p(\cdot)$ can be employed as a substitute of $\mathbb{I}(\cdot)$ to describe objective functions [16]. Given G_j and budget k , we use $O(\hat{G}_j; k)$ to denote the value of objective function in equation (5)/(6) when using up all budget k (e.g., in equation (5), $O(\hat{G}_j; k) = \mathbb{I}\left(f_\theta(\hat{G}_j) \neq y_j\right)$ or $p\left(f_\theta(\hat{G}_j) \neq y_j\right)$).

4 PROPOSED APPROACH

Our projective ranking method mainly includes the ranking module and the projection module. In this section, we first formulate the perturbation space and propose the principles of our evaluation framework. Then we present the detail of the ranking module and the perturbation projection operation. Finally, we give an algorithm to show the generation of adversarial samples.

4.1 Attack Setting

In our method, given a victim model f_θ , we assume that the attackers can have access to the nodes embedding and predictive probability distribution of f_θ to learn the attack strategy. Then, only accessing the embedding of nodes, the attackers may utilize the learned strategy to attack any samples of the victim model under any budget setting.

To further explore the transferability of the learned strategy (in Section 6.5), we assume an intelligent attacker attempts to fool the victim models by accessing the nodes embedding of the target models based on the attack strategy learned from the other source models engaged in the similar data domain. We note that the attacker does not know any other knowledge (like the architecture or parameters of the target models) except for the embedding of nodes. This scenario reflects the vulnerability of the models that use the pre-training models [35].

4.2 Perturbation Space

In an evasion attack, an attacker \mathcal{T} can perturb a clean sample G to obtain an adversarial sample \hat{G} . We formulate the process of this perturbation on graph G as

$$\hat{G} = \mathcal{T}_f(G) = G + \Delta G, \quad (7)$$

where $\Delta G = \{\Delta A, \Delta X\}$ is the perturbation graph. To be more precise, the graph structure and node features of \hat{G} are expressed as

$$\begin{aligned} \{\hat{A}, \hat{X}\} &= \{A + \Delta A, X + \Delta X\}, \\ \Delta A &= m_A \odot [\mathbb{I}(add) \cdot (I_A - A) + \mathbb{I}(del) \cdot (-A)], \\ \Delta X &= m_X \odot (I_X - 2X), \end{aligned} \quad (8)$$

where $A \in \{0, 1\}^{|\mathcal{V}| \times |\mathcal{V}|}$ is the adjacency matrix, $X \in \{0, 1\}^{|\mathcal{V}| \times d}$ is binary node features matrix, $I_A = J_{|\mathcal{V}|} - I_{|\mathcal{V}|}$, $I_X = J_{|\mathcal{V}|, d}$ (J is the all-ones matrix, I is the identity matrix). $|\mathcal{V}|$ is the number of nodes in G , and d is the size of node features. $m_A \in \{0, 1\}^{|\mathcal{V}| \times |\mathcal{V}|}$ and $m_X \in \{0, 1\}^{|\mathcal{V}| \times d}$ represent the masks of graph structure and node features respectively. $\mathbb{I}(add)/\mathbb{I}(del)$ is the indicator function to show if adding/deleting edge operation is allowed in generating adversarial samples. \odot is the Hadamard product and \cdot is the scalar multiplication. Therefore, the perturbation graph $\Delta G = \{\Delta A, \Delta X\}$ is actually defined by the combination of specified structure mask m_A and feature mask m_X . The similarity measure function in (5) and (6) is refined as

$$\mathcal{I}(\hat{G}, G) = \mathbb{I}(a\|m_A\|_1 + \|m_X\|_1 \leq k), \quad (9)$$

where $\|\cdot\|_1$ is the L1 Norm, k is the budget of perturbations. a is a scalar coefficient, and it is 1 if G is a directed graph

and $\frac{1}{2}$ otherwise since the adjacency matrix of undirected graph is symmetric.

Given the clean sample G , the *perturbation space* $\mathbb{T}(G)$ of G is defined as the set of all possible perturbation graph $\Delta G = \{\Delta A, \Delta X\}$. The *size* of a perturbation graph ΔG is defined as:

$$\|\Delta G\| = a\|m_A\|_1 + \|m_X\|_1 \in \mathbb{Z}_0^+, \quad (10)$$

where \mathbb{Z}_0^+ is the set of non-negative integer. In the *perturbation space* $\mathbb{T}(G)$, the operators \odot and $+$ on perturbation graphs are defined as:

$$\begin{aligned} \Delta G_\alpha \odot \Delta G_\beta &= \{\Delta A_\alpha \odot \Delta A_\beta, \Delta X_\alpha \odot \Delta X_\beta\}, \\ \Delta G_\alpha + \Delta G_\beta &= \{\lceil \Delta A_\alpha + \Delta A_\beta \rceil, \lceil \Delta X_\alpha + \Delta X_\beta \rceil\}, \end{aligned}$$

where $\lceil \cdot \rceil$ means the elements of the input matrix is limited in $[-1, 1]$. The *perturbation space* $\mathbb{T}(G)$ with budget k is defined as

$$\mathbb{T}_k(G) = \{\Delta G \mid \|\Delta G\| = k\}. \quad (11)$$

Specially, we call $\Delta G \in \mathbb{T}_1(G)$ an *operation element* of *perturbation space* $\mathbb{T}(G)$.

Given the above definitions and operators, the *perturbation space* $\mathbb{T}(G)$ owns the following properties:

Property 1. If $\Delta G_0 \in \mathbb{T}_0(G)$, then $\forall \Delta G_\alpha \in \mathbb{T}_m(G)$, we have

$$\begin{aligned} \Delta G_0 \odot \Delta G_\alpha &= \Delta G_0, \\ \Delta G_0 + \Delta G_\alpha &= \Delta G_\alpha. \end{aligned} \quad (12)$$

Property 2. Given $\Delta G_\alpha, \Delta G_\beta \in \mathbb{T}_1(G)$, $\Delta G_\alpha \odot \Delta G_\beta \in \mathbb{T}_1(G)$ if $\alpha = \beta$, otherwise $\Delta G_\alpha \odot \Delta G_\beta \in \mathbb{T}_0(G)$.

Property 3. $\forall \Delta G_\alpha \in \mathbb{T}_m(G)$, $\Delta G_\beta \in \mathbb{T}_n(G)$, we have $\Delta G_\alpha + \Delta G_\beta \in \mathbb{T}_{m+n-\|\Delta G_\alpha \odot \Delta G_\beta\|}(G)$.

Proof: Given the definition of $\mathbb{T}_k(G)$, the result is a direct consequence of the following calculations. Based on the definition of $+$ and \odot operation, we have

$$\begin{aligned} \|\Delta G_\alpha + \Delta G_\beta\| &= \|\Delta G_\alpha\| + \|\Delta G_\beta\| - \|\Delta G_\alpha \odot \Delta G_\beta\| \\ &= m + n - \|\Delta G_\alpha \odot \Delta G_\beta\| \end{aligned}$$

Property 4. Given $\Delta G_\alpha \in \mathbb{T}_1(G)$, $\Delta G_\beta \in \mathbb{T}_{\kappa-1}(G)$ ($\kappa \in \mathbb{Z}^+$), $\Delta G_\alpha + \Delta G_\beta \in \mathbb{T}_\kappa(G)$ if $\Delta G_\alpha \odot \Delta G_\beta \in \mathbb{T}_0(G)$.

Based on property 4, it is easy to obtain that the *perturbation space* $\mathbb{T}_k(G)$ is actually composed of k different *operation elements* of $\mathbb{T}(G)$, which means that

$$\begin{aligned} \mathbb{T}_k(G) &= \{\Delta G \mid \Delta G = \sum_{\kappa=1}^k \Delta G_{\kappa}; \Delta G_{\kappa} \in \mathbb{T}_1(G), \\ &\quad \Delta G_{\kappa_i} \odot \Delta G_{\kappa_j} \in \mathbb{T}_0(G), \forall \kappa_i \neq \kappa_j\}, \end{aligned} \quad (13)$$

and the *size* of $\mathbb{T}_k(G)$ is

$$|\mathbb{T}_k(G)| = C_E^k, \quad E = |\mathbb{T}_1(G)|, \quad (14)$$

where $|\cdot|$ is the size of a set, and C is the combination operation of two integers.

4.3 Projective Ranking

4.3.1 Design Goal and Principles in Evaluation Framework

In this section, we consider a fundamental expectation of the adversary as the **design goal** of evasion attack methods: *An intelligent attacker always expects to choose the perturbation operation which will bring the most significant attack benefit at each perturbation step for achieving stealthy and effective attacks.*

Assuming that $O(\hat{G}; k) = \sum_{i=1}^k B(\Delta G_i)$, where $\Delta G_i \in \mathbb{T}_1(G)$ and $\sum_{i=1}^k \Delta G_i \in \mathbb{T}_k(G)$. $B(\cdot)$ is the attack benefit function defined on ΔG_i , $B(\Delta G_i)$ presents the contribution of ΔG_i to $O(\hat{G}; k)$. At each perturbation step, the design goal can be formulated as

$$\arg \max_{\Delta G_i} B(\Delta G_i). \quad (15)$$

A. From Design Goal to Evaluation Framework

To achieve the above expectation, we propose an evaluation framework to reveal its core requirements. Our framework composed of three principles, they are:

(1) **Benefit decomposition.** Defining the attack benefit of perturbation operation is the first step to achieving the expectation. When budget $k > 1$, perturbations at each step are combined together to function as a whole. Although final attack results come from collaboration of k different $\Delta G \in \mathbb{T}_1(G)$, only one $\Delta G \in \mathbb{T}_1(G)$ can be chosen at each perturbation step. This fact requires that the attack benefit $B(\cdot)$ should be felicitously defined on $\Delta G \in \mathbb{T}_1(G)$ to support the intelligent attacker making perturbation decision.

To this end, $B(\Delta G)$ should be formulated as a contribution distribution function of $O(\hat{G}; k)$ (see Section 3.3) on $\Delta G \in \mathbb{T}_1(G)$. For example, when using Shapley value ϕ [36] as the contribution distribution function, $B(\Delta G) = \phi(\Delta G | O(\hat{G}; k))$. In this paper, an attack method satisfies the *benefit decomposition* principle if it considers all perturbations as a whole to evaluate their attack results, and uses some mechanisms to distribute the overall benefit to the perturbations at each step.

(2) **Baseline graph.** When defining $B(\cdot)$, an implicit ground object is that the *baseline graph* of attack benefit should be fixed on the clean graph G , i.e., $B(\cdot) = B(\cdot|G)$, and $B(\Delta G) = 0$ where $\|\Delta G\| = 0$. If the baseline graph changes to other graphs, the measure of attack benefit will deviate from the original meaning (see the example of *GradArgmax* in Appendix B).

(3) **Operation ranking.** To achieve stealthy and effective evasion attacks, given specific values of $B(\cdot)$ on $\Delta G \in \mathbb{T}_1(G)$, an intelligent attacker should choose the perturbation with maximal attack benefit in each step. In the above process, the intelligent attacker ranks $\Delta G \in \mathbb{T}_1(G)$ according to their attack benefits, and then choose top- k different perturbation operations one-by-one. In this paper, an attack method satisfies the *operation ranking* principle if its perturbation at each step consumes the attack budget by considering the $B(\cdot)$ -based ranking of $\Delta G \in \mathbb{T}_1(G)$.

B. From Evaluation Framework to Our Method

In this section, we utilise principles in the evaluation framework and additional requirements to guide the design of our method. Generally, an intelligent attacker always attempts to maximise the profits in attacks (see Appendix A). In this paper, we extend the definition of *transferability* of attack

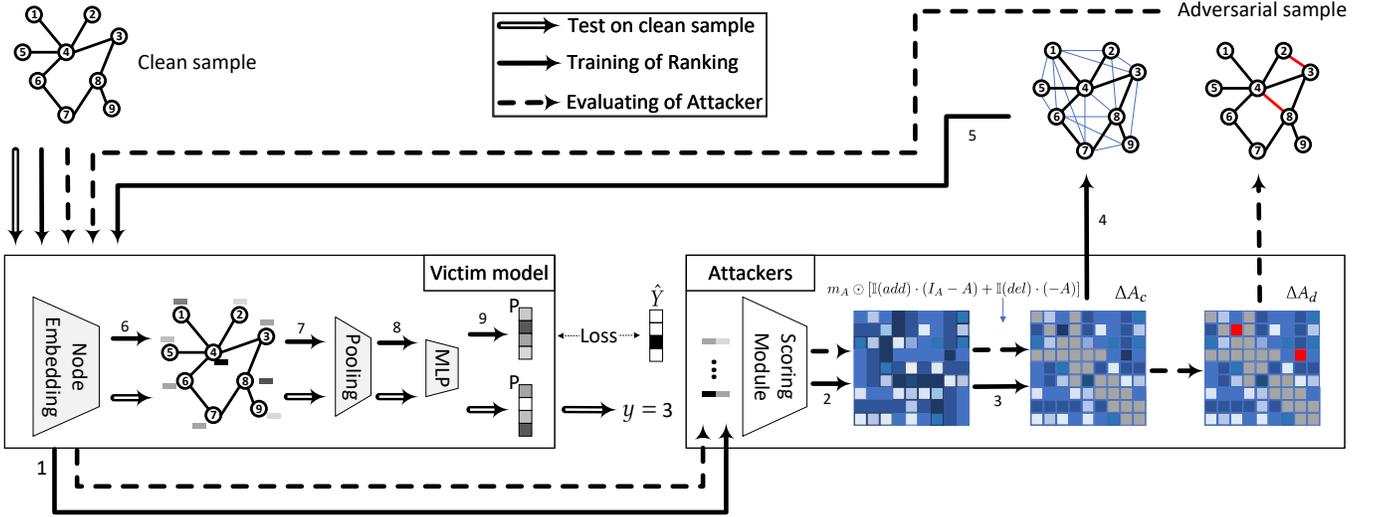


Fig. 1. Illustration of the projective ranking method. The victim model f_θ can make the correct prediction on a clean sample G (shown in hollow arrows). During the scoring module training (shown in the steps 1-9 with solid arrows), the attacker \mathcal{T}_f employs the mutual information between the perturbation space $\mathbb{T}(G)$ and the attacker's goal $y_{\hat{G}} \neq y_G$ to measure and rank the importance of all elements in $\mathbb{T}(G)$. The scoring module needs access node embedding and predictive probability distribution of the victim model. In the evaluation phase (shown in dashed arrows), the attacker \mathcal{T}_f only needs to access the node embedding to obtain the ranking of the elements in $\mathbb{T}(G)$, and then projects the *operation ranking* to generate adversarial sample \hat{G} under the specified budget.

strategies. The *transferability* means that once attackers learn the attack strategies, they can generate adversarial samples for unseen clean samples under different perturbation budgets. However, if attack strategies are learned from fixed budget k (e.g., *RL-S2V*), these strategy cannot easily satisfy *transferability* since they are designed for specific k . Therefore, the evaluation framework and desired transferability practically require an attack method accomplishes $B(\cdot)$ -based ranking of $\Delta G \in \mathbb{T}_1(G)$ without considering specific k in $B(\cdot)$.

To get rid of the limitation of specific k , we employ all perturbation operation $\Delta G \in \mathbb{T}_1(G)$ of the clean graph G (i.e., *baseline graph*) as a whole to attack target GNNs. Based on mutual information, the $B(\cdot)$ of each ΔG is then calculated as their importance (see more in Appendix B) for final attack results. In this way, our method satisfies the *benefit decomposition* principle. To satisfy the *operation ranking* principle, we first rank $\Delta G \in \mathbb{T}_1(G)$ according to their importance values (i.e., attack benefit), and then project this ranking into practical attacks with specific k .

4.3.2 Ranking method

Now, given a clean sample G as the baseline graph, attackers attempt to rank all operation elements in perturbation space $\mathbb{T}(G)$ with respect to their importance. Inspired by the interpretability research of GNNs [37], we measure the importance of elements in $\mathbb{T}_1(G)$ by mutual information (MI) between the modified graph \hat{G} and the attacker's goal. It can be expressed as:

$$\max \mathbf{MI}(\hat{Y}, \hat{G}) = H(\hat{Y}) - H(\hat{Y}|\hat{G}), \quad (16)$$

where $H(\cdot)$ is the entropy function. In untargeted evasion attacks, $\hat{Y} = (\dots, p_{y_G} = 0, \dots)$ is the expected prediction distribution of \hat{G} , y_G is the original category of G . For the clean sample G , the first item in (16) is a constant since

the victim model f_θ is fixed and \hat{Y} is also invariant. So the objective in (16) is equal to

$$\min H(\hat{Y}|\hat{G}). \quad (17)$$

To reduce the computational difficulties caused by the discrete graph structure, we apply continuous relaxation on ΔG and assume it is a graph variable $\Delta G \sim \mathcal{T}_f(G)$. Based on Jensen's inequality and $H(\cdot)$ is a concave function, we obtain that

$$\begin{aligned} H(\hat{Y}|\hat{G}) &= \sum_{\Delta G \sim \mathcal{T}_f(G)} p(\Delta G) H(\hat{Y}|G + \Delta G) \\ &= E_{\Delta G} [H(\hat{Y}|G + \Delta G)] \\ &\leq H(\hat{Y}|G + E[\Delta G]), \end{aligned} \quad (18)$$

where $E[\cdot]$ is expectation function. So the objective (17) is equal to

$$\min_{\mathcal{T}_f(G)} H(\hat{Y}|G + E_{\mathcal{T}_f(G)}[\Delta G]). \quad (19)$$

To be more specific, given the victim model f_θ , the objective of the untargeted evasion attacks is

$$\min_{\mathcal{T}_f(G)} - \sum_y \mathbb{I}(y \neq y_G) \log p(y|\hat{G}), \quad (20)$$

where $p(\cdot|\hat{G})$ is the predictive probability distribution of f_θ on \hat{G} . The objective of the targeted evasion attacks is

$$\min_{\mathcal{T}_f(G)} - \sum_y \mathbb{I}(y = y_t) \log p(y|\hat{G}), \quad (21)$$

where y_t is the specified target category.

Following the attack setting in previous methods [21], we assume that attackers are only able to add edges when generating \hat{G} . So we have

$$\hat{G} = \mathcal{T}_f(G) = \{A + \Delta A, X\}, \quad (22)$$

where $\Delta A = m_A \odot (I_A - A)$, the mask m_A is obtained by

$$\begin{aligned} m_{A_{i,j}} &= s(h_i, h_j) \\ &= \text{softmax}(MLP(\text{concat}(h_i, h_j))), \end{aligned} \quad (23)$$

where h_i is the embedding of node i , $s(\cdot, \cdot)$ is the scoring function which measures the importance of elements in $\mathbb{T}_1(G)$ with respect to the attacker’s expectation. In our method, after concatenating the embedding of nodes v_i and v_j , a Multi Layer Perceptron (MLP) model and the softmax function are employed to obtain the final score. Since the value of ΔA is a real number rather than a discrete value, we call \hat{G} is generated by adding continuous structure perturbations $\Delta G_c = \{\Delta A_c, 0\}$.

4.3.3 Perturbation Projection

In our method, the learned attack strategy is embedded in the ranking of $\Delta G = \{\Delta A, \Delta X\} \in \mathbb{T}_1(G)$. Due to the discrete structure limitation of graph data, although attackers could obtain the adversarial sample \hat{G} in (22) by adding the continuous perturbation ΔG_c , it is necessary to bridge the gap between continuous perturbation ΔG_c and discrete modification ΔG_d under limited budgets, Inspired by Projected Gradient Descent (PGD) algorithm, we map ΔG_c to ΔG_d by below projection function

$$\Delta A_{d;i,j} = \mathbb{I}(\Delta A_{c;i,j} \in \text{topk}(\Delta A_c, k)), \quad (24)$$

where k is the perturbation budget, $\text{topk}(\cdot, k)$ is the set of $\Delta A_{c;i,j}$ with top-k values, i and j indicate the element at i -th row and j -th column of matrix. By this projection, attackers obtain the adversarial sample $\hat{G} = \{A + \Delta A_d, X\}$ from clean sample G under specified budget k . Figure 1 illustrates the pipeline of our projective ranking method.

After obtaining the adversarial samples $\hat{D} = \{\hat{G}^m\}_{m=1}^M$, the attacker use them to attack the victim model f_θ . Algorithm 1 shows how attackers generate adversarial samples from clean samples \mathcal{D} by our projective ranking method. To learn an attack strategy, in line 6, attackers first need to obtain the embedding representation of all nodes h of clean samples in \mathcal{D} from the victim model f_θ . In the training phase (lines 9-12), attackers use the scoring function in equation (23) to obtain structure mask m_A , then obtain the perturbations on graph structure ΔA_c by limiting m_A with the allowed perturbation operation type. Then, in line 11, attackers add perturbations ΔA_c to the clean samples to generate a relaxed adversarial sample \hat{G}_c . In line 12, attackers use the objective (20) to learn an attack strategy embedded in the scoring function. In the evaluation phase (lines 13-18), attackers will obtain the practical adversarial sample \hat{G}_d to evaluate the attack performance of the learned attack strategy. In line 14, attackers project the learned ranking into the practical attack space, in which attackers are only allowed to add edges with the specified budget ($k = 1$). Then attackers obtain the final adversarial samples in line 15 and attack the victim model in line 17. Attackers will repeat the process (lines 9-18) until the projective ranking method learned a high attack strategy. By replacing the objective in line 12 with objective (21), attackers could obtain the adversarial samples under the setting of targeted attacks.

Algorithm 1: Generation of Adversarial Samples

Input: $\mathcal{D} = \{G^m = \{A^m, X^m\}\}_{m=1}^M$, classifier f_θ
Output: $\hat{D} = \{\hat{G}^m = \{A^m, X^m\}\}_{m=1}^M$
Parameters: φ //The trainable parameters of s
Initialization: $h = \text{NodeEmbed}(\mathcal{D}|f_\theta)$,
 $ASR_{best} = 0, k = 1$

- 1 **Def** Ranking (\mathcal{D}):
- 2 **for** ($m = 1; m \leq M; m = m + 1$)
- 3 $S_{i,j}^m = s_\varphi(h_i^m, h_j^m)$
- 4 $\Delta A_c^m = (I_{A^m} - A^m) \odot S^m$
- 5 **return** $\{\{\Delta A_c^m\}_{m=1}^M\}$
- 6 $h = \text{NodeEmbed}(\mathcal{D}|f_\theta)$, $ASR_{best} = 0, k = 1$
- 7 **Function** Main:
- 8 **while** (*not* *EarlyStop*)
- 9 // Attacker Training
- 10 $\{\Delta A_c^m\} = \text{Ranking}(\mathcal{D})$
- 11 $\{\hat{G}_c^m\} = \{\{A^m + \Delta A_c^m, X^m\}\}$
- 12 $\min_\varphi - \sum_{m=1}^M \sum_y \mathbb{I}(y \neq y_G) \log p(y|\hat{G}_c^m)$
- 13 // Attacker Evaluation
- 14 $\{\Delta A_d^m\} = \text{topk}(\text{Ranking}(\mathcal{D}))$
- 15 $\hat{D} = \{\{A^m + \Delta A_d^m, X^m\}\}$
- 16 // Update the Attack Success Rate
- 17 **if** ($ASR(\hat{D}|f_\theta) > ASR_{best}$)
- 18 $ASR_{best} = ASR_{current}$

TABLE 2
Consistency with the Principles of the Evaluation Framework

method	benefit decomposition	baseline graph	operation ranking
Random	○	●	○
GradArgmax	○	○	○
RL-S2V	●	●	○
Our	●	●	●

○ means neglect, ● means consideration.

5 METHOD ANALYSIS UNDER OUR EVALUATION FRAMEWORK

In this section, we use the three principles in Section 4.3.1 to make an evaluation on our method and three typical attack methods: *RandomSampling*, *GradArgmax* and *RL-S2V*. The results are summarized in the Table 2. In these methods, *RandomSampling* only satisfies the *baseline graph* principle, our method satisfies the *attack benefit*, *operation ranking* and *baseline graph* simultaneously. The other methods are partially consistent with the evaluation framework. The reasons are as follows.

(1) GradArgmax. Similar to the use of gradient descent for training in neural networks, *GradArgmax* employs the gradient of f_θ on all *operation elements* $\Delta G_{cur} \in \mathbb{T}_1(G_{cur})$ to choose perturbation operation, where G_{cur} is the graph waiting to be modified at the current perturbation step. Hence, *GradArgmax* neglects the *baseline graph* principle. To use up all perturbation budget k , attackers need to calculate the gradient information at each perturbation step. Then it will use the real-time local gradient as the measure of attack

TABLE 3
Datasets Statistics

Dataset	# of Graphs	# of Classes	Avg. # of Edges
ENZYMES	600	6	62.14
Mutagenicity	4337	2	30.77
PC-3	27509	2	28.49
NCI109	4127	2	32.13
NCI-H23H	26838	2	37.27
BA-2Motifs	1,000	2	25.48

benefits. Actually, the gradient information is a measure of modification sensitivity (see Appendix B), so *GradArgmax* does not satisfy the *attack benefit* principle. To generate adversarial samples, *GradArgmax* focuses on integrating all perturbation graph $\Delta G_{cur} \in \mathbb{T}_1(G_{cur})$, which owns the biggest local benefit at each perturbation step. Although the operations in *GradArgmax* have an order, it does not satisfy the *operation ranking* principle since the local gradient information is not a suitable measure for attack benefits.

(2) **RL-S2V**. In the generation of adversarial samples, *RL-S2V* uses the attack benefit of $\Delta G \in \mathbb{T}_k(G)$ to decide the perturbation operation $\Delta G \in \mathbb{T}_1(G)$ of each step in consuming perturbation budget k . The reward function in *RL-S2V* is designed by considering the outputs of the victim model f_θ on \hat{G} and G , so it satisfies the *baseline graph* and *attack benefit* requirements. However, it emphasizes using $\Delta G \in \mathbb{T}_k(G)$ as a whole perturbation to attack the victim model f_θ with specified budget k , while cares less about the order of the element $\Delta G \in \mathbb{T}_1(G)$ that composes the perturbation space $\mathbb{T}(G)$. Hence, the *RL-S2V* attack method neglects the *attack ranking*.

Furthermore, we analyze the difference between the measures of attack benefits (sensitivity, long-term benefit, importance) in the Appendix B. We also show the weakness of *GradArgmax* concerning the attack benefits from three different aspects and empirically demonstrate them in our experimental results.

6 EXPERIMENTS

6.1 Datasets and Baselines

We employ several real-world datasets ENZYMES, Mutagenicity, PC-3, NCI109, NCI-H23H [38] and one synthesized dataset BA-2Motifs [39] for graph classification. For the NCI-H23H dataset, we only choose the graphs whose node size is less than 50. Table 3 shows some basic statistics of these datasets.

To evaluate the performance of our method, we select *RandomSampling*, *GradArgmax*, and *RL-S2V* [21] as baselines. In the *RandomSampling* method, we performed ten times with different seeds and then averaged these accuracy results. In our experiments, the attack performance is measured by the accuracy of the victim model, in which a low accuracy number indicates a high attack performance.

6.2 Experimental Setup

In the victim models, we randomly split each dataset into training data (80%), validation data (10%), and test data (10%) to train the victim GAT [40] or GCN [41] models. The victim models have three hidden layers, with 20 as the output feature dimension. We concatenate the *maxpooling*

and *sumpooling* results of the final embedding of nodes to obtain the expression of the whole graph, then use a fully connected layer to predict the category of the graph. In our projective ranking method, we use a 2-layers MLP to serve as the scoring module.

To evaluate the *transferability* of our method, we directly project the learned strategy under $k = 1$ to the generation of adversarial samples under $k = 2, 3$. The other results are obtained by running corresponding attack methods under a specified budget, respectively.

6.3 Attack Performance Comparison

6.3.1 Untargeted Attacks

The upper half of Table 4 and 5 show the accuracy of the victim model f_θ on both clean and adversarial samples generated by different attack methods. The bold numbers indicate the best attack results under the same setting.

In Table 4 and 5, our method achieves the best or competitive attack performance on all datasets with $k=1$, indicating the projective ranking method owns *powerful* attack performance. When $k=2$ or 3, we use the learned attack strategy under $k=1$ to generate adversarial samples for the changed perturbation budget. The results show our method also obtain the best or competitive attack effect, which shows that the projective ranking method has learned an effective *transferable* attack strategy under budget $k=1$.

GradArgmax generates the adversarial examples based on the gradient of the victim model and makes a greedy choice in each step. The attack results of *GradArgmax* in the Table 4 and 5 empirically prove our discussion about sensitivity in Appendix B. Firstly, the perturbation generated by *GradArgmax* is sub-optimal since the gradient is the sensitivity measure of the victim model. Although the *GradArgmax* achieves effective attack performance on the victim GCN model, its ability on the victim GAT model is limited (see Figure 2). Secondly, the result on the NCI109 dataset with $k=1$ in Table 5 shows the *GradArgmax* generates samples with negative attack performance. This indicates that its attack performance is limited by the non-linear nature of the GNN model in some situations. Finally, the attack performance of *GradArgmax* is worse than the *RandomSampling* on ENZYMES, PC-3 and NCI109 datasets when $k=2$ and 3, on which *GradArgmax* shows weak marginal attack performance concerning the budget. Moreover, the *GradArgmax* does not learn any attack strategy in the attack process. Above results indicate that *GradArgmax* is not desirable for attackers in some situations since it misses the *baseline graph* and *attack benefit* principles in evasion attacks.

Compare with using the “local” gradient in *GradArgmax*, *RL-S2V* and our method achieve stable attack performance on both GAT and GCN models since both of them consider the *importance* of perturbation operation with “global” criteria. We also use *RandomSampling* as a baseline to evaluate other attack methods. Table 4 and 5 show our method always achieve better attack performance than *RandomSampling*. The *italic* shows unexpected results in the aspect of attack ability, where the performance of *RL-S2V* is worse than *RandomSampling* on ENZYMES ($k=2,3$) in Table 4 and ENZYMES ($k=3$), NCI109 ($k=3$) in Table 5. Moreover, attackers always expect to obtain better attack

TABLE 4

Classification Accuracy of the Victim GAT Model (%). The upper half shows the attack results of different attack methods on seen samples, and the lower half shows the attack results on unseen samples. k is the perturbation budget.

Dataset	ENZYMES			Mutagenicity			PC-3			NCI109			NCI-H23H		
k	1	2	3	1	2	3	1	2	3	1	2	3	1	2	3
Clean	65.83	65.83	65.83	73.63	73.63	73.63	51.75	51.75	51.75	76.50	76.50	76.50	71.25	71.25	71.25
Rand*	60.04	51.71	45.79	73.39	70.86	69.08	<i>51.85</i>	51.74	51.55	74.80	71.25	68.50	70.80	66.48	63.80
Grad*	<i>65.83</i>	<i>65.83</i>	<i>65.83</i>	<i>73.63</i>	<i>73.63</i>	<i>73.63</i>	<i>51.75</i>	<i>51.75</i>	<i>51.75</i>	<i>76.50</i>	<i>76.50</i>	<i>76.50</i>	<i>71.25</i>	<i>71.25</i>	<i>71.25</i>
RL-S2V	53.75	<u>52.08</u>	<u>51.46</u>	69.38	68.25	68.50	51.13	51.13	50.75	69.88	68.13	67.25	62.38	62.50	60.50
Ours	48.75	39.17	33.13	71.88	69.63	68.25	51.50	51.25	51.00	67.75	63.38	60.13	62.87	55.13	49.25

Transfer Attack of the Learned Strategy on Unseen Samples															
Dataset	ENZYMES			Mutagenicity			PC-3			NCI109			NCI-H23H		
k	1	2	3	1	2	3	1	2	3	1	2	3	1	2	3
Clean	64.17	64.17	64.17	75.74	75.74	75.74	95.60	95.60	95.60	78.18	78.18	78.18	84.54	84.54	84.54
Rand	63.08	58.08	53.33	74.78	72.59	71.02	95.60	95.58	95.56	76.69	73.14	70.42	82.99	80.05	77.40
Grad	-	-	-	-	-	-	-	-	-	-	-	-	-	-	-
RL-S2V	59.17	<u>59.17</u>	<u>58.33</u>	73.42	<u>73.17</u>	<u>72.43</u>	95.59	<u>95.59</u>	<u>95.62</u>	74.99	<u>73.82</u>	<u>72.26</u>	81.75	<u>81.12</u>	76.72
Ours	63.33	52.50	45.83	74.72	71.67	69.52	95.60	95.57	95.54	71.90	67.18	63.81	77.92	72.34	66.56

* Rand is the *RandomSampling* attack method, and Grad is the *GradArgmax* attack method.

TABLE 5

Classification Accuracy of the Victim GCN Model (%). The upper half shows the attack results of different attack methods on seen samples, and the lower half shows the attack results on unseen samples. k is the perturbation budget.

Dataset	ENZYMES			Mutagenicity			PC-3			NCI109			NCI-H23H		
k	1	2	3	1	2	3	1	2	3	1	2	3	1	2	3
Clean	69.17	69.17	69.17	85.25	85.25	85.25	67.13	67.13	67.13	76.50	76.50	76.50	64.75	64.75	64.75
Rand	64.81	56.33	51.23	80.80	75.56	70.75	64.60	60.10	57.64	73.83	67.60	63.29	60.06	55.26	53.51
Grad	64.79	<u>61.46</u>	<u>58.13</u>	68.13	54.50	45.50	<u>66.13</u>	<u>65.38</u>	<u>65.25</u>	<u>77.00</u>	<u>74.00</u>	<u>71.00</u>	56.13	53.25	52.63
RL-S2V	58.54	56.04	<u>55.42</u>	71.88	69.50	63.75	57.88	55.88	55.00	66.00	65.00	<u>64.13</u>	54.38	52.88	52.00
Ours	52.50	44.79	42.92	67.63	59.13	53.63	56.13	52.13	49.62	68.38	59.00	56.75	53.13	50.25	50.13

Transfer Attack of the Learned Strategy on Unseen Samples															
Dataset	ENZYMES			Mutagenicity			PC-3			NCI109			NCI-H23H		
k	1	2	3	1	2	3	1	2	3	1	2	3	1	2	3
Clean	69.17	69.17	69.17	84.93	84.93	84.93	96.37	96.37	96.37	78.45	78.45	78.45	98.41	98.41	98.41
Rand	66.83	59.67	54.25	81.01	75.62	70.81	95.69	94.57	93.39	76.17	70.23	65.70	98.34	98.14	97.99
Grad	-	-	-	-	-	-	-	-	-	-	-	-	-	-	-
RL-S2V	63.33	<u>62.50</u>	<u>61.67</u>	74.39	74.07	66.95	<u>95.75</u>	<u>95.58</u>	<u>94.91</u>	74.03	<u>72.47</u>	<u>69.40</u>	98.30	97.69	97.63
Ours	60.00	51.67	44.17	74.44	63.84	57.45	95.11	93.14	91.74	74.12	67.33	63.63	98.23	97.82	97.55

performance when giving more budgets. If the budget increases, a well-designed attack method should not decrease its performance. However, like the result in [23], we also observed that the attack performance of *RL-S2V* degrade when increasing the perturbation budget on Mutagenicity ($k=3$) in Table 4. This may be due to the less effectiveness of the Q-learning method in *RL-S2V*, especially for the Markov decision process with a long horizon.

6.3.2 Targeted Attacks

We also conduct targeted attacks on the ENZYME dataset. Without loss of generality, these methods attempt to attack GNN models so that they classify graphs from other classes (i.e., 1-5) as class 0. The upper half of Table 6 shows the

attack success rate of different attack methods, and our method far outperforms other baselines in attack performance. Moreover, in targeted attacks, we also found the same weaknesses of *GradArgmax* and *RL-S2V* that they have in untargeted attacks (see *italic* results).

Remarks. When training GAT model on the NCI-H323H dataset, we employ undersampling on the category with most samples to alleviate the unfavourable effect caused by unbalanced distribution. In the training data, the # of positive samples: # of Negative samples = 1:2.

All results in this section are achieved by directly applying attack methods on the vanilla GNN models. Recently, the randomized smoothing method [42], [43] has

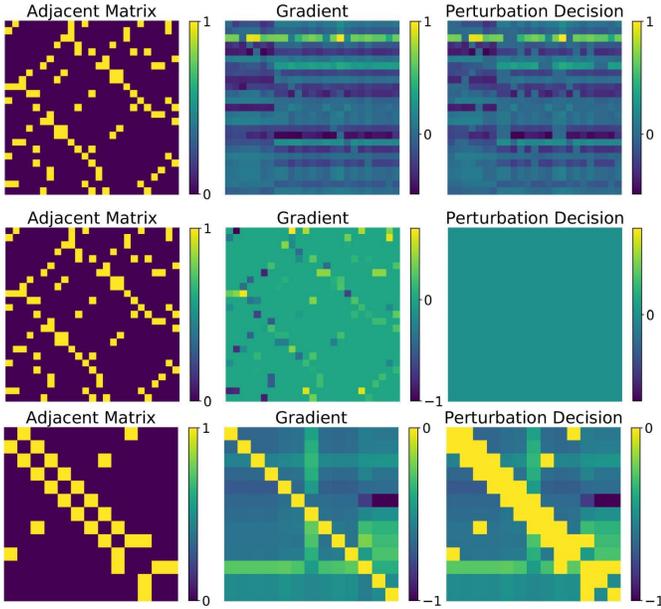


Fig. 2. Visualization of the graph structure, gradient information and perturbation decision in *GradArgmax*. The 1st and 2nd rows of images come from the same sample under the GCN and GAT models, respectively. Compared with the victim GCN model, the nonzero gradients from the GAT model almost locate at the same position as the graph structure. The zero-gradient at the location of all possible edge adding operations invalidates the *GradArgmax* attack method on the victim GAT model. The 3rd row of images is a sample based on the GCN model. Although this sample has nonzero perturbation decision values on the edge adding positions, the decision value is negative. Adding edges on this kind of sample is also unavailable since adding edges on any position causes negative attack results. In this figure, we have scaled the values in the middle and right columns to [-1,1] for better visualisation.

TABLE 6
Attack Success Rate (%) of Targeted Attacks on ENZYMES.

Model	GCN			GAT		
k	1	2	3	1	2	3
Rand	2.03	4.45	7.53	2.45	5.60	7.90
Grad	4.50	10.75	15.75	<u>0.00</u>	<u>0.00</u>	<u>0.00</u>
RL-S2V	7.25	9.50	9.50	5.50	6.25	<u>5.25</u>
Ours	10.75	16.00	19.25	9.50	14.75	17.50

Transfer Attack of the Learned Strategy on Unseen Samples						
k	1	2	3	1	2	3
Rand	1.40	2.80	5.00	2.10	4.20	4.60
Grad	-	-	-	-	-	-
RL-S2V	3.00	6.00	<u>4.00</u>	3.00	<u>4.00</u>	<u>1.00</u>
Ours	7.00	9.00	14.00	8.00	15.00	18.00

been widely employed to improve the robustness of AI models. In this paper, we follow the setting (noise parameter $\beta = 0.9/0.7$, sampling number $d = 10000$) of recent research on certified robustness of GNNs [44] to evaluate the attack performance of our method. Experimental results show randomized smoothing [44] is an effective defence method. However, for GNN models in this paper, randomized smoothing is not applicable because it significantly degrades the performance (i.e., accuracy) of GNNs. For example, as shown in Table 7, although our method almost cannot attack the GCN models on ENZYMES/Mutagenicity

after introducing randomized smoothing, the accuracy of GCN equipped with the defence method ($\beta = 0.9$) on clean graphs is only 22.29%/53.00%, which is dramatically lower than that of vanilla GCN models suffering attacks with $k = 1$ (i.e., 52.50%/67.63%).

TABLE 7
Accuracy (%) Comparison of the Victim Models without/with Defence.

Dataset		ENZYMES			Mutagenicity		
	k	1	2	3	1	2	3
W/o*	Clean	69.17	69.17	69.17	85.25	85.25	85.25
	Ours	52.50	44.79	42.92	67.63	59.13	53.63
W*	Clean	22.29	22.29	22.29	53.00	53.00	53.00
	Ours	22.29	22.29	22.29	52.37	52.13	52.00
W	Clean	17.50	17.50	17.50	49.13	49.13	49.13
	Ours	17.50	17.50	17.50	49.25	49.00	49.00

* W/o indicates results on vanilla GCN models, and W indicates results on GCN models equipped with randomized smoothing. β presents the noise parameter in the randomized smoothing.

6.4 Transferability on Unseen Samples

To reduce attackers' effort to generate adversarial samples from unseen clean samples, they generally expect a transferable attack strategy. In this section, we use the attack strategies obtained in Section 6.3 to generate adversarial samples for unseen samples and then employ them to attack the victim models.

6.4.1 Untargeted Attacks

The lower half of Table 4 and 5 show the classification accuracy of f_θ on both clean and adversarial samples. We consider the *RL-S2V* and our projective ranking method since only they can learn transferable attack strategies. The bold results indicate the best method under the same setting, and *italic* show unexpected results in the aspect of transferable attack performance. Firstly, the results in Table 4 and 5 show both *RL-S2V* and our method could use the learned attack strategy to generate effective adversarial samples under perturbation budget $k=1$ on all datasets. It indicates that the learned strategy can be transferred to attack unseen samples. Secondly, the results under $k=2, 3$ further demonstrate that the projective ranking method owns transferable attack performance on unseen samples when the budget changes. Especially, our method obtains the best attack performance on some datasets when $k=2$ or 3 even if it does not own the best performance when $k=1$. Finally, compared with *RandomSampling*, the transferability of the attack strategy of *RL-S2V* is limited on most datasets when $k=2$ or 3, maybe the *RL-S2V* did not learn a powerful attack policy when $k > 1$. These results reveal that the victim models make consistent mistakes at both the sample and the budget levels. The attackers can utilize this fact to learn the attack strategy only under a specific budget with limited resources and then use the attack strategies to attack the target classifiers when the attack scenario changes.

6.4.2 Targeted Attacks

The lower half of Table 6 shows attack success rate of attack methods on unseen samples. Attack results show

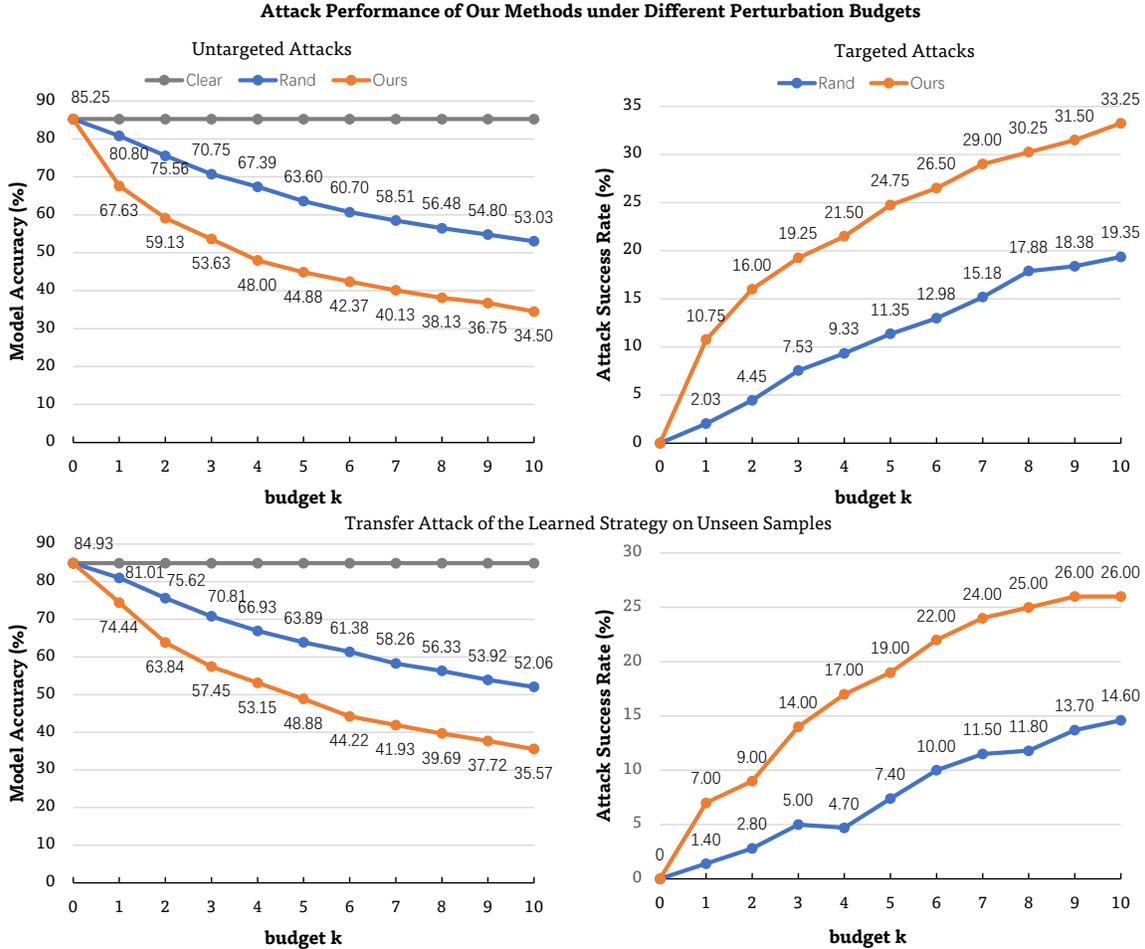


Fig. 3. Attack performance of our methods under different perturbation budgets. The figures in the left/right column show untargeted/targeted attack results (i.e., model accuracy, or attack success rate) on Mutagenicity/ENZYMES dataset. The figures in the first/second row show attack results on seen/unseen samples.

TABLE 8
Classification Accuracy of the Victim GAT/GCN Model (%).

Dataset	ENZYMES			Mutagenicity			PC-3			NCI109			NCI-H23H		
k	1	2	3	1	2	3	1	2	3	1	2	3	1	2	3
Clean	65.83	65.83	65.83	73.63	73.63	73.63	51.75	51.75	51.75	76.50	76.50	76.50	71.25	71.25	71.25
Rand	60.04	51.71	45.79	73.39	70.86	69.08	<u>51.85</u>	51.74	51.55	74.80	71.25	68.50	70.80	66.48	63.80
GCN-GAT*	57.50	49.38	44.17	71.25	65.88	62.88	51.50	51.38	51.25	75.25	70.50	67.13	69.38	66.38	63.75

Dataset	ENZYMES			Mutagenicity			PC-3			NCI109			NCI-H23H		
k	1	2	3	1	2	3	1	2	3	1	2	3	1	2	3
Clean	69.17	69.17	69.17	85.25	85.25	85.25	67.13	67.13	67.13	76.50	76.50	76.50	64.75	64.75	64.75
Rand	64.81	56.33	51.23	80.80	75.56	70.75	64.60	60.10	57.64	73.83	67.60	63.29	60.06	55.26	53.51
GAT-GCN	56.04	43.96	36.46	80.63	74.13	68.63	62.50	58.75	55.50	68.00	62.00	57.75	56.75	51.88	50.75

* This means we use the adversarial sample generated from the GCN model to attack the victim GAT model.

our method observably outperforms *RandomSampling* and *RL-S2V*. Moreover, in targeted attacks, the transferability of attack strategy from *RL-S2V* is also limited (see *italic* results) when comparing with *RandomSampling*.

6.5 Other Transferability Evaluations

6.5.1 Transferability on Attack Budget

Figure 3 shows the attack performance of our method on seen samples under different attack budgets. The performance curves illustrate our method learned effective and

transferable attack strategies in untargeted and targeted attacks. Moreover, Figure 3 also empirically demonstrates that our method satisfies the *operation ranking* principle in the evaluation framework since smaller budgets own larger marginal attack performance.

6.5.2 Transferability on Victim Model

To further explore the transferability, we use the adversarial samples generated from GCN/GAT model to attack the victim GAT/GCN model. The attack results are shown in

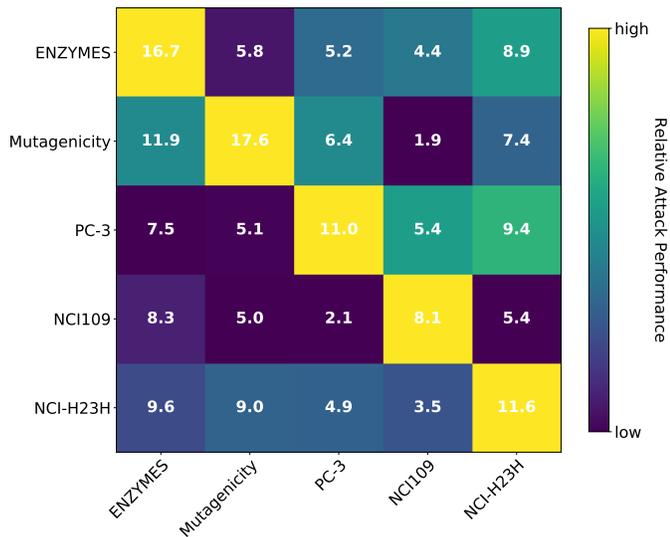


Fig. 4. Visualization of transferable attack performance ($k=1$). The row is the dataset on which the source attacker is trained, and the column is the dataset of the target GCN model. These numbers indicate how much the classification accuracy of the target classifiers have decreased, and a higher value means a stronger attack capability. The color indicates the relative attack performance.

Table 8, and these adversarial samples achieve better attack performance than *RandomSampling*. It indicates these victim models used for the same task on the same dataset may make consistent mistakes to some extent.

6.5.3 Transferability on Data Domain

This evaluation explores the transferability of the attack strategy learned on one dataset to attack the victim models built on other datasets. We visualized the attack results on the victim GCN model in Figure 4. Firstly, the relative attack performance’s colour indicates that when the source attacker and the target model have the same dataset, it achieves the best attack performance. Secondly, since the graphs in all datasets are small molecules or come from bioinformatics, the result values in Figure 4 show the domain similarity of these graphs brings non-negative attack performance.

These results reveal the potential risk of employing a pre-training model with a freezing setting [35] in the downstream tasks. In Figure 4, we observe that when attacking the NCI-H23H dataset using the attack strategy from the ENZYMES dataset, the accuracy performance drops 8.9%, which is larger than that of *RandSampling* (4.7%) and *GradArgmax* (8.6%). Once the adversary knows the victim model $f(\theta)$ uses the pre-training model f_{emb} , they could train a classifier $f'(\phi)$ on graphs $G_{f'}$ that come from the same domain of the data G_f in $f(\theta)$, then use the attack strategy learned on $f'(\phi)$ and the embedding of G_f from f_{emb} to attack the victim models.

6.6 Visualization of Attack Patterns

To reveal the attack strategies of the projective ranking method, we visualize the perturbations in adversarial samples on the BA-2Motifs dataset based on the GCN model. BA-2Motifs is a synthetic dataset in which two motifs (*House* and *Pentagon*) are attached on random base graphs. Table 9 shows the attack results of different methods.

TABLE 9
Classification Accuracy of the Victim Model (%) on BA-2Motifs.

k	current samples			unseen samples		
	1	2	3	1	2	3
Clean	99.63	99.63	99.63	100.00	100.00	100.00
Rand	78.85	54.35	50.09	81.00	55.35	50.00
Grad	60.50	51.13	50.13	-	-	-
RL-S2V	50.00	50.00	50.00	50.00	50.00	50.00
Ours	50.00	50.00	50.00	50.00	50.00	50.00

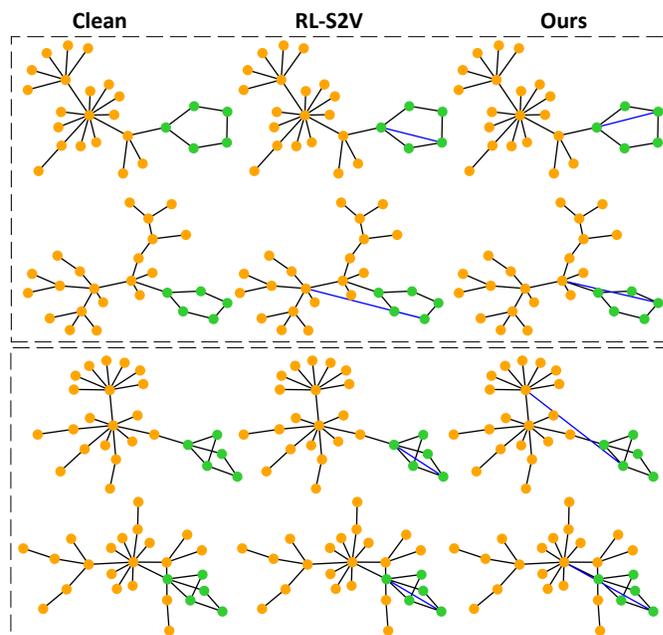


Fig. 5. Visualization of adversarial samples. The graphs in the left column are clean samples, and the subgraphs in first/second block composed of green nodes are the motif "Pentagon"/"House". The graphs in the middle and right column are adversarial samples generated by *RL-S2V* and our method, respectively. In this figure, the attackers attempt to fool the victim models to predict "House"/"Pentagon" on the adversarial samples in first/second block. Both *RL-S2V* and our method present two attack patterns: **imitation of other motifs** and **collapse of self-motif**.

In untargeted evasion attacks, we found two fundamental strategies in the generation of the adversarial samples. They are: (1) *placing the adversarial samples in the high-confidence region of the other categories in the victim models*, and (2) *moving the clean samples to the classification boundary or other low-confidence areas of the victim models*. We dive into the adversarial samples and observe some enlightening attack patterns in them:

Imitation of other motifs. In the first row of the first block in Figure 5, both *RL-S2V* and our method add one edge in the *Pentagon* so that there is a *House* in the adversarial samples. In this way, the victim GCN model classifies the adversarial samples as *House* graphs.

Collapse of self-motif. In the second row of the first block and the second block in Figure 5, both *RL-S2V* and our method attack the victim model by adding one edge in which one node is in the self-motif. In this way, the attackers destroy the self-motif pattern by moving the samples to the low-confidence areas to fool the victim model.

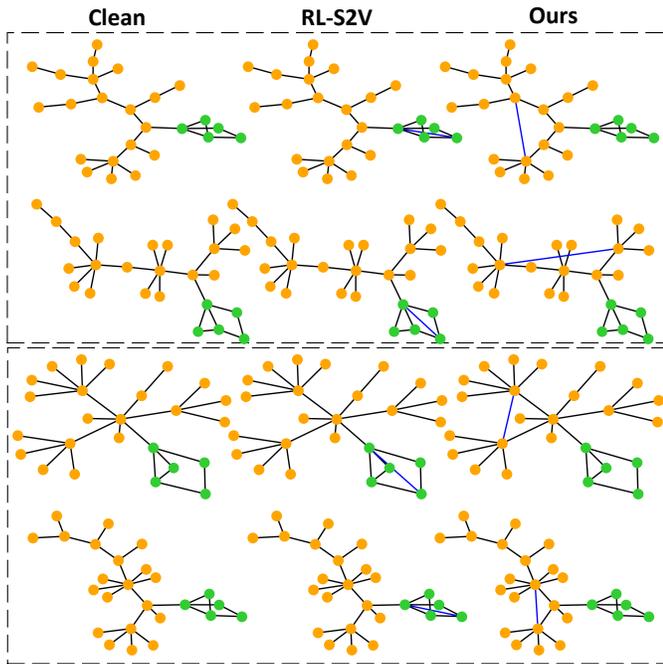


Fig. 6. Visualization of adversarial samples. Compared with *RL-S2V*, our method presents various attack patterns. They are the **coexistence of motifs** (first block) and the **fake self-motif** (second block).

Although the attack results in Table 9 indicate *RL-S2V* and our method have the same attack performance, we find the attack patterns of *RL-S2V* are simple and lack variation from the second column in both Figure 5 and 6. However, another two attack patterns are found in our method:

Coexistence of motifs. In the first block of Figure 6, our method shows a new attack pattern. One edge is added between two nodes that are outside of the self-motif in the clean samples. The exciting part of this edge is that the distance of the two end-nodes of it is 5, and after this perturbation operation, there is a motif *Pentagon* in these samples. The coexistence of motifs is regarded as one behaviour that belongs to the second strategy in generating adversarial samples, in which the clean samples are moved to the decision boundary of the victim models.

Fake self-motif. In the second block of Figure 6, our method adds one edge between two nodes outside of the self-motif, resulting in one triangle constructed in the adversarial samples. As a critical part of the *House* motif, the constructed triangle could confuse the victim models since two “similar” self-motifs exist in current samples. In this way, the samples are moved from the high-confidence region of the victim model to the low-confidence area.

In this section, we visualize the adversarial samples and summarize two basic attack strategies in them. We also found four attack patterns—imitation of other motifs, the collapse of self-motif, coexistence of motifs, and fake self-motif—of the adversarial samples. Compared with the *RL-S2V*, the adversarial samples generated by the projective ranking method show various attack patterns. These attack patterns are helpful for the adversary to find the graph pattern differences between different data classes. Based on these observations, the attackers can customize the pattern operation to obtain adversarial samples of the specified type of clean graph samples.

7 CONCLUSION

In this paper, we present the projective ranking approach to perform an evasion attack for graph classification. We contend that current evasion approaches either do not provide adequate attack performance without considering the perturbations’ long-term benefits or require attackers to readjust the attack strategies when the attack environment changes. To that purpose, we define the perturbation space and propose an evaluation framework on the evasion attacks for graph classification. Then we first relax perturbation space for ranking its elements based on mutual information, and then we project the ranking into generating adversarial samples with a specified budget. The experimental results show that our method performs well in attack performance, and the learned attack strategies can be directly transferred to generate adversarial samples when the budget changes. Furthermore, the visualization of adversarial samples generated by our method shows a variety of attack patterns, which helps identify the vulnerability of the victim models.

Our future works include simultaneously making perturbations in structure and node features and performing evasion attacks on directed graphs and graphs with edge attributes. In addition, we will dive into the attack patterns of adversarial samples to explore the link between the robustness and interpretability of the target models.

ACKNOWLEDGEMENT

This research was supported in part by an ARC Future Fellowship (No. FT210100097) and the National Natural Science Foundation of China (No. 61872360).

REFERENCES

- [1] T. Ma, C. Xiao, J. Zhou, and F. Wang, “Drug similarity integration through attentive multi-view graph auto-encoders,” in *IJCAI*, 2018.
- [2] S. Fortunato, C. T. Bergstrom, K. Börner, J. A. Evans, D. Helbing, S. Milojević, A. M. Petersen, F. Radicchi, R. Sinatra, B. Uzzi *et al.*, “Science of science,” *Science*, 2018.
- [3] C. Zheng, X. Fan, S. Pan, Z. Wu, C. Wang, and P. S. Yu, “Spatio-temporal joint graph convolutional networks for traffic forecasting,” *arXiv:2111.13684*, 2021.
- [4] M. Jin, Y. Zheng, Y.-F. Li, S. Chen, B. Yang, and S. Pan, “Multivariate time series forecasting with dynamic graph neural ODEs,” *arXiv:2202.08408*, 2022.
- [5] X. Zheng, Y. Liu, S. Pan, M. Zhang, D. Jin, and P. S. Yu, “Graph neural networks for graphs with heterophily: A survey,” *arXiv:2202.07082*, 2022.
- [6] M. Jin, Y. Zheng, Y.-F. Li, C. Gong, C. Zhou, and S. Pan, “Multi-scale contrastive siamese networks for self-supervised graph representation learning,” in *IJCAI*, 2021.
- [7] M. Wu, S. Pan, and X. Zhu, “Openwgl: open-world graph learning for unseen class node classification,” *KAIS*, 2021.
- [8] B. Xiong, S. Zhu, N. Potyka, S. Pan, C. Zhou, and S. Staab, “Semi-riemannian graph convolutional networks,” *arXiv:2106.03134*, 2021.
- [9] Y. Liu, Z. Li, S. Pan, C. Gong, C. Zhou, and G. Karypis, “Anomaly detection on attributed networks via contrastive self-supervised learning,” *TNNLS*, 2021.
- [10] Y. Zheng, M. Jin, Y. Liu, L. Chi, K. T. Phan, S. Pan, and Y.-P. P. Chen, “From unsupervised to few-shot graph anomaly detection: A multi-scale contrastive learning approach,” *arXiv:2202.05525*, 2022.
- [11] J. Gao, J. Gao, X. Ying, M. Lu, and J. Wang, “Higher-order interaction goes neural: A substructure assembling graph attention network for graph classification,” *TKDE*, 2021.

- [12] Z. Liu, Y. Fang, Y. Liu, and V. W. Zheng, "Neighbor-anchoring adversarial graph neural networks," *TKDE*, 2021.
- [13] P. Li, Y. Wang, H. Wang, and J. Leskovec, "Distance encoding: Design provably more powerful neural networks for graph representation learning," in *NerualIPS*, 2020.
- [14] J. Liu, F. Xia, L. Wang, B. Xu, X. Kong, H. Tong, and I. King, "Shifu2: A network representation learning based model for advisor-advisee relationship mining," *TKDE*, 2019.
- [15] J. Li, H. Peng, Y. Cao, Y. Dou, H. Zhang, P. Yu, and L. He, "Higher-order attribute-enhancing heterogeneous graph neural networks," *TKDE*, 2021.
- [16] W. Jin, Y. Li, H. Xu, Y. Wang, S. Ji, C. Aggarwal, and J. Tang, "Adversarial attacks and defenses on graphs," in *SIGKDD*, 2020.
- [17] L. Chen, J. Li, J. Peng, T. Xie, Z. Cao, K. Xu, X. He, and Z. Zheng, "A survey of adversarial learning on graphs," *arXiv:2003.05730*, 2020.
- [18] B. Wu, X. Yang, S. Pan, and X. Yuan, "Adapting membership inference attacks to GNN for graph classification: Approaches and implications," in *ICDM*, 2021.
- [19] L. Sun, Y. Dou, C. Yang, J. Wang, P. S. Yu, L. He, and B. Li, "Adversarial attack and defense on graph data: A survey," *arXiv:1812.10528*, 2018.
- [20] B. Wu, X. Yang, S. Pan, and X. Yuan, "Model extraction attacks on graph neural networks: Taxonomy and realization," in *AsiaCCS*, 2022.
- [21] H. Dai, H. Li, T. Tian, X. Huang, L. Wang, J. Zhu, and L. Song, "Adversarial attack on graph structured data," in *ICML*, 2018.
- [22] D. Zügner, A. Akbarnejad, and S. Günnemann, "Adversarial attacks on neural networks for graph data," in *SIGKDD*, 2018.
- [23] Y. Ma, S. Wang, T. Derr, L. Wu, and J. Tang, "Graph adversarial attack via rewiring," in *SIGKDD*, 2021.
- [24] R. Ying, J. You, C. Morris, X. Ren, W. L. Hamilton, and J. Leskovec, "Hierarchical graph representation learning with differentiable pooling," in *NerualIPS*, 2018.
- [25] Y. Ma, S. Wang, C. C. Aggarwal, and J. Tang, "Graph convolutional networks with eigenpooling," in *SIGKDD*, 2019.
- [26] Z. Zhang, J. Bu, M. Ester, J. Zhang, C. Yao, Z. Yu, and C. Wang, "Hierarchical graph pooling with structure learning," *arXiv:1911.05954*, 2019.
- [27] H. Tang, G. Ma, Y. Chen, L. Guo, W. Wang, B. Zeng, and L. Zhan, "Adversarial attack on hierarchical graph pooling neural networks," *arXiv:2005.11560*, 2020.
- [28] X. Wang, M. Cheng, J. Eaton, C.-J. Hsieh, and F. Wu, "Attack graph convolutional networks by adding fake nodes," *arXiv:1810.10751*, 2018.
- [29] H. Wu, C. Wang, Y. Tyshetskiy, A. Docherty, K. Lu, and L. Zhu, "Adversarial examples for graph data: Deep insights into attack and defense," in *IJCAI*, 2019.
- [30] A. Bojchevski and S. Günnemann, "Adversarial attacks on node embeddings via graph poisoning," in *ICML*, 2019.
- [31] M. Fang, G. Yang, N. Z. Gong, and J. Liu, "Poisoning attacks to graph-based recommender systems," in *ACSAC*, 2018.
- [32] Z. Zhang, J. Jia, B. Wang, and N. Z. Gong, "Backdoor attacks to graph neural networks," in *SACMAT*, 2021.
- [33] Z. Xi, R. Pang, S. Ji, and T. Wang, "Graph backdoor," in *USENIX*, 2021.
- [34] J. Gilmer, S. S. Schoenholz, P. F. Riley, O. Vinyals, and G. E. Dahl, "Neural message passing for quantum chemistry," in *ICLR*, 2017.
- [35] W. Hu, B. Liu, J. Gomes, M. Zitnik, P. Liang, V. S. Pande, and J. Leskovec, "Strategies for pre-training graph neural networks," in *ICLR*, 2020.
- [36] X. Wang, J. Ren, S. Lin, X. Zhu, Y. Wang, and Q. Zhang, "A unified approach to interpreting and boosting adversarial transferability," in *ICLR*, 2021.
- [37] R. Ying, D. Bourgeois, J. You, M. Zitnik, and J. Leskovec, "Gnnexplainer: Generating explanations for graph neural networks," in *NerualIPS*, 2019.
- [38] C. Morris, N. M. Kriege, F. Bause, K. Kersting, P. Mutzel, and M. Neumann, "Tudataset: A collection of benchmark datasets for learning with graphs," in *ICML*, 2020.
- [39] D. Luo, W. Cheng, D. Xu, W. Yu, B. Zong, H. Chen, and X. Zhang, "Parameterized explainer for graph neural network," in *NerualIPS*, 2020.
- [40] P. Velickovic, G. Cucurull, A. Casanova, A. Romero, P. Liò, and Y. Bengio, "Graph attention networks," in *ICLR*, 2018.
- [41] T. N. Kipf and M. Welling, "Semi-supervised classification with graph convolutional networks," in *ICLR*, 2017.
- [42] J. M. Cohen, E. Rosenfeld, and J. Z. Kolter, "Certified adversarial robustness via randomized smoothing," in *ICML*, 2019.
- [43] J. Jia, X. Cao, B. Wang, and N. Z. Gong, "Certified robustness for top-k predictions against adversarial perturbations via randomized smoothing," in *ICLR*, 2020.
- [44] B. Wang, J. Jia, X. Cao, and N. Z. Gong, "Certified robustness of graph neural networks against adversarial structural perturbation," in *SIGKDD*, 2021.
- [45] W. Hu, B. Liu, J. Gomes, M. Zitnik, P. Liang, V. Pande, and J. Leskovec, "Strategies for pre-training graph neural networks," in *ICLR*, 2020.
- [46] M. Sundararajan, A. Taly, and Q. Yan, "Gradients of counterfactuals," *arXiv:1611.02639*, 2016.
- [47] Sundararajan, Mukund and Taly, Ankur and Yan, Qiqi, "Axiomatic attribution for deep networks," in *ICML*, 2017.
- [48] H. Wu, C. Wang, Y. Tyshetskiy, A. Docherty, K. Lu, and L. Zhu, "Adversarial examples for graph data: Deep insights into attack and defense," in *IJCAI*, 2019.

APPENDIX A

CHALLENGES IN EVASION ATTACK

Unlike attack methods for node classification and link prediction, we find some challenges in designing evasion attack methods for graph classification. They are:

(1) Huge search space. The perturbation space is huge when the size of graph data is big. For example, it is hard for attackers to obtain the optimal adversarial samples when making edge perturbations. Different from mainly considering the link situation of the target node in the node-level task, the time complexity in the graph-level attack tasks is $O(n^2)$, where n is the node number of the graph. When d -dimension binary attributes are associated with edges [45], this complexity changes to worse $O(2^d n^2)$. It is usually difficult for the adversary to solve this discrete combinatorial optimization problem.

(2) Profits maximization. The profits here include the direct and indirect profits. The direct profit is the attack benefit since the primary goal of attackers is to obtain adversarial samples with high attack performance. The indirect profits contain learning transferable strategies and defect mining. In the aspect of transferable strategies, attackers expect to learn strategies that help attack unseen samples or generate adversarial samples under a changed perturbation budget. In the aspect of defect mining, the adversary yearns for revealing the defects or weaknesses of the victim models by analyzing the patterns in adversarial samples. The weaknesses of the victim models inspire attackers in designing more powerful attack methods. Once the flaws of the victim models are found, they could customize the attack strategies for different types of data to improve the attack performance.

APPENDIX B

DIFFERENT MEASURES OF ATTACK BENEFIT

In this section, we will discuss the measure differences between *sensitivity*, *long-term benefit*, and *importance* concerning the *attack benefit* principle.

B.1 Sensitivity

The sensitivity here refers to the gradient in the *GradArgmax* method. It is intuitional to employ the gradient to make perturbation decision, since the gradient in *GradArgmax*

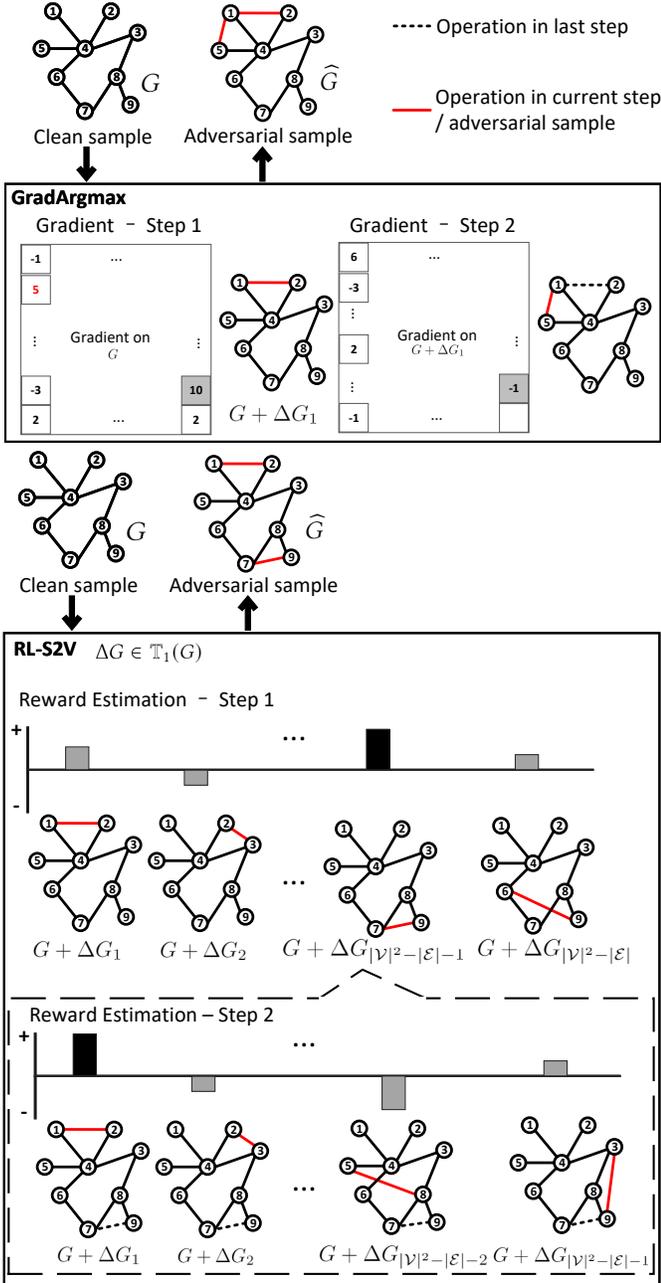


Fig. 7. Illustration of *GradArgmax* and *RL-S2V*. *GradArgmax* uses real-time gradient information to make perturbations, *RL-S2V* utilizes the estimated long-term benefits to finish the attack.

method exactly describe the structure or feature sensitivity of graph G with respect to the victim model f_θ . Taking the edge perturbation on graph G as example, a coefficient $a_{u,v}$ is introduced for each nodes pair $(u, v) \in \mathcal{V} \times \mathcal{V}$, and $a_{u,v} = \mathbb{I}(v \in N(u))$. The message function in (2) changes to

$$m_u^{t+1} = \sum a_{u,v} M_t(h_u^t, h_v^t, e_{uv}). \quad (25)$$

To generate an adversarial sample, attackers first need to calculate the gradient on all $a_{u,v}$

$$g_{u,v} = \frac{\partial \mathcal{L}}{\partial a_{u,v}}, \quad (26)$$

where \mathcal{L} is the loss function of victim models. Then *GradArgmax* will choose the position with the largest positive $g_{u,v}$ to add an edge or the smallest negative $g_{u,v}$ to remove an edge. *GradArgmax* will repeat the above process until it uses up all perturbation budget k .

However, the gradient which measures the *sensitivity* is not suitable enough to measure the **importance** of each perturbation operation for some reasons [46], [47], [48]:

(1) The perturbation generated by *GradArgmax* is sub-optimal. The principle in *GradArgmax* is choosing the position with gradient extremum to make modifications. If there is an edge at the position with the largest positive gradient value or there is no edge at the position with the smallest negative gradient value, *GradArgmax* will have to re-select the perturbation position.

(2) The non-linear nature of GNN models limits the attack performance of *GradArgmax*. In *GradArgmax*, attackers expect to predict the change of loss function on every single operation with

$$\begin{aligned} B(\cdot | f_\theta) &= \mathcal{L}_k - \mathcal{L}_{k-1} = \Delta \mathcal{L} \\ &= \mathcal{L}(G + \Delta G) - \mathcal{L}(G) \\ &\approx \langle \nabla G \mathcal{L}(G), \Delta G \rangle \\ &= \sum g_{u,v} \Delta A_{u,v}, \end{aligned} \quad (27)$$

which is only a first-order linear approximation function about ΔG . However, to obtain powerful discrimination ability, GNN models usually contain nonlinear activation functions like ReLU. The linear approximation based on local gradient can't describe the change in the output of the victim models well when the input value changes greatly. Since the values in the adjacency matrix are discrete, the change from 0 to 1 or 1 to 0 may far exceeds the predictive ability of the above approximation. Taking $y(x) = \text{Relu}(x)$ as example, the gradient at $x = 0$ is $g(0) = 0$. When x changes from 0 to 1, $y(1) - y(0) \approx g(0)(1 - 0) = 0$ is far from the ground-truth $y(1) - y(0) = 1$.

(3) The iterative selection of perturbation operations based on local gradients cannot accurately describe the attacker's expectations. The *GradArgmax* attempts to use the local gradient to approximately measure the importance of each perturbation operation in the generation of adversarial samples. When the perturbation budget $k > 1$, the local gradient is not a suitable approximate measure. The reason is the local gradient $g_{u,v}$ at the κ^{th} ($1 < \kappa \leq k$) perturbation step is calculated based on current graph which is obtained by adding a perturbation graph $\Delta G \in \mathbb{T}_{\kappa-1}(G)$. Actually, in the κ^{th} perturbation step, the attackers attempt to choose the perturbation operation which brings κ^{th} largest attack benefit for the original clean sample G , but not the operation that brings 1^{st} largest benefit for current graph $G + \Delta G$ ($\Delta G \in \mathbb{T}_{\kappa-1}(G)$). So the gradient information is enough to predict the *sensitivity* but not a suitable measure to identify the *importance* of each operation.

B.2 Long-term Benefit

The *long-term benefit* here is the estimated reward of each operation in the adversarial samples generated by reinforcement learning. A conspicuous drawback of *GradArgmax* is that the greedy selection mechanism focuses on the short-term benefit (i.e., maximizing loss function) of the current

operation, while neglect the benefit of current operation should be defined by its importance in final adversarial samples. In the training of *RL-S2V* with perturbation budget k , the estimated reward of each perturbation operation is 0 when the perturbation budget k is not used up. Once the budget is exhausted, the adversarial samples obtain positive or negative reward defined by the output of the victim model f_θ on these samples. In the experience pool of *RL-S2V*, the *long-term benefit* of each perturbation operation is determined by the final benefit of adversarial samples. In this way, *RL-S2V* can learn a more powerful attack strategy than *GradArgmax*.

B.3 Importance

The reward function in *RL-S2V* mainly focuses on the overall benefits caused by all perturbation operations in the adversarial samples. The *long-term benefit* of each perturbation operation in *RL-S2V* can only be evaluated by the reward function after the generation of adversarial examples exhausts all perturbation budget k . The *long-term benefit* reflects the *absolute importance* of each perturbation operation according to the reward function under a specific budget k . This kind of absolute importance of the same perturbation operation is different under various perturbation budgets in attack methods based on reinforcement learning [21], [23], so *RL-S2V* needs retraining to obtain attack strategy when the perturbation budget changes. From the perspective of *operation ranking* principle, compared with the specific *absolute importance* of each perturbation operation, attackers are more concerned about which perturbation operation should be selected from the perturbation space (i.e., *relative importance*).